International Journal of Sensors

Research Article
Published: 28 May, 2019

Electro-Mechanical Impedance (EMI) based Axial Loads Influence on Damage of Steel Fiber Concrete

Dongdong Chen[1], Zhijie Wang[2#], Hao Cheng[1], Linsheng Huo[1] and Gangbing Song[3]**

[1]Key Laboratory of Coastal and Offshore Engineering, Dalian University of Technology, China

[2]Department of Underground Engineering, School of Civil Engineering, Southwest Jiaotong University, China

[3]Department of Mechanical Engineering, Smart Materials and Structures Laboratory, University of Houston, USA

[#]The co-first author who has equal contribution with the first author

Abstract

Steel fiber concrete has higher tensile strength, higher fatigue strength and higher fracture toughness than traditional reinforced concrete. Because of these advantages, it is one of the most widely used types of material in water resources and hydropower engineering. In this paper, the Smart Aggregate (SA) sensors which made by sandwiched the water proofed piezoceramic patch into protective materials were casted into the steel fiber concrete specimens. The steel fiber concrete, which average compressive strength is 50 MPa, are divided into five groups according to different content of steel fiber (0, 30, 60, 90, 120) (kg/m^3). Based on the electro-mechanical impedance signal which acquired from the Smart Aggregate (SA), the cracks and the damage status of steel fiber concrete can be detected. Specifically, the effects of axial compressive load were investigated by using step-by-step loading scheme which includes elastic, plastic and the destruction loading stage. A normalized Root-Mean-Square Deviation (RMSD) based analysis was developed to determine the relationship between destruction and impedance signal. The test results show that the normalized RMSD impedance damage index increases gradually with the increase of axial loading. It can be used to monitor the damage status of steel fiber concrete.

Keywords: Health monitoring; Steel fiber concrete; Axial loads; Impedance method; Smart aggregate

OPEN ACCESS

Correspondence:

Linsheng Huo, Key Laboratory of Coastal and Offshore Engineering, Dalian University of Technology, Dalian, 116024, China,

E-mail: lshuo@dlut.edu.cn

Gangbing Song, Department of Mechanical Engineering, Smart Materials and Structures Laboratory, University of Houston, Houston, Texas, 77204, USA,

E-mail: gsong@uh.edu

Received Date: *20 Apr 2019*

Accepted Date: *21 May 2019*

Published Date: *28 May 2019*

Citation:

Chen D, Wang Z, Cheng H, Huo L, Song G. Electro-Mechanical Impedance (EMI) based Axial Loads Influence on Damage of Steel Fiber Concrete. Int J Sens. 2019; 1(1): 1002.

Copyright *© 2019 Linsheng Huo and Gangbing Song. This is an open access article distributed under the Creative Commons Attribution License, which permits unrestricted use, distribution, and reproduction in any medium, provided the original work is properly cited.*

Introduction

In recent years, steel fiber concrete has been widely used in high-rise buildings, long-span bridges and hydropower structures [1], because of its improved properties in tensile strength, fatigue strength and fracture toughness [2,3]. Therefore, the entire service period structural health monitoring of steel fiber concrete structures become much more important. The application of high-performance intelligent material sensors in damage detection has become the trend of structural health monitoring. Among them, smart aggregate as the representative for smart materials have been widely used in structural damage detection for its good mechanical and electrical coupling properties. During past few years, the electro-mechanical impedance technique has become a new promising method in crack detection and structure health monitoring and it has been widely used in aerospace and aircraft structures [4-6], civil engineering [7] and so on.

Song et al. [8] proposed the concept of embeddable piezoceramic based "smart aggregate" for health monitoring of concrete structures. Initially, Gu et al. [9] applied smart aggregate to the early strength monitoring of concrete. By establishing the empirical relationship between the amplitude of the signal received by the sensor and the experimental strength of the concrete, the early compressive strength of the concrete was effectively predicted. Song et al. [10] applied smart aggregate to detect an over-height truck collision with a concrete bridge. The smart aggregates also have been used to identify internal cracks effectively in reinforced concrete structures by using the active sensing [11]. Experiments show that the wavelet packet analysis method can effectively identify the development of concrete cracks. And then, the feasibility of using smart aggregate to monitor the internal stress of a structure was verified by Du et al. [12].

Electro-mechanical impedance method, which originated in the 1990s, is a novel health monitoring technology which can detect the internal damage of the structure by analyzing the structural vibration characteristics. In 1993, Liang et al. [13] first proposed the electro-

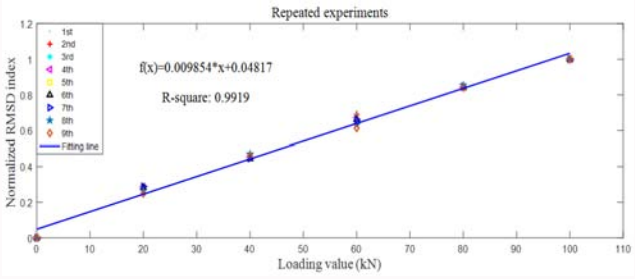

Figure 1: Linear fitting of nine repeated experiments.

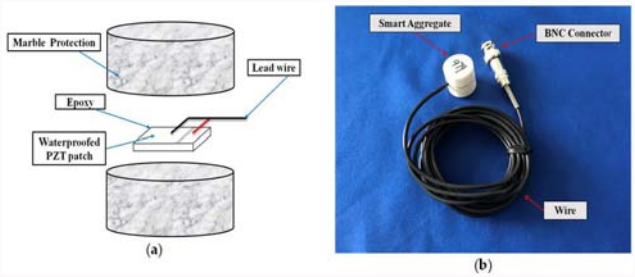

Figure 2: Smart aggregate, (a) The design scheme of Smart aggregate; (b) The structure of smart aggregate.

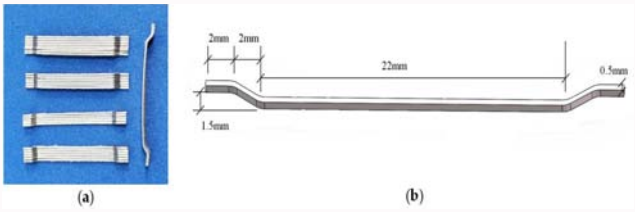

Figure 3: Steel fiber, (a) The photo of steel fibers; (b) The size of steel fiber.

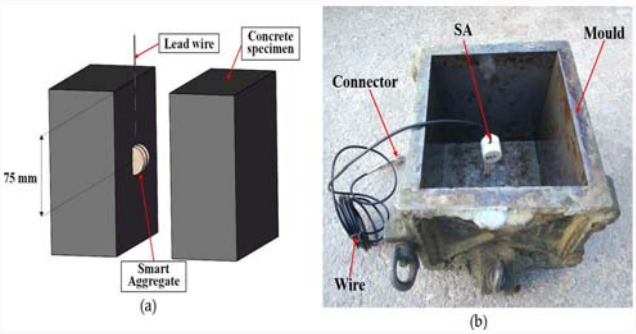

Figure 4: Smart aggregate placement schematic, (a) Smart aggregate placement schematic; (b) Smart aggregate placement photos.

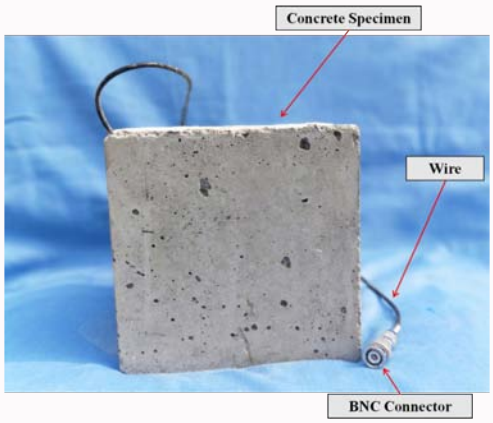

Figure 5: Specimen photos.

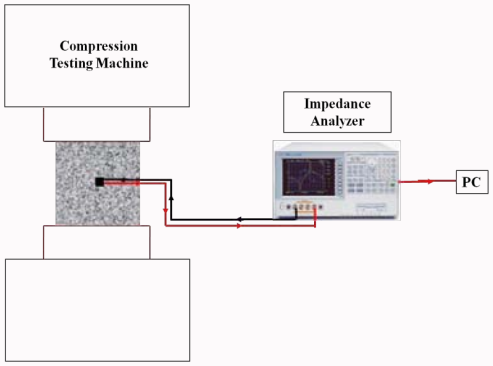

Figure 6: The testing schematic.

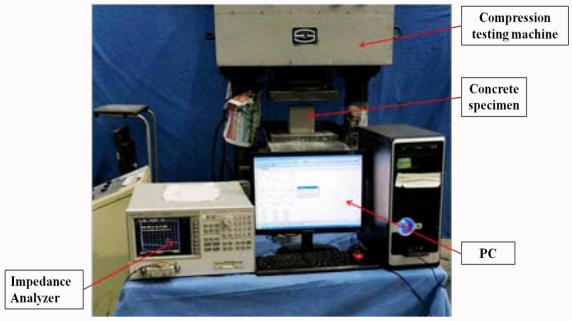

Figure 7: The testing devices.

mechanical impedance method for structures with a piezoceramic transducer. After that, Liang et al. [14] used EMI to study actuator power consumption and system energy transfer. Later Liang et al. [15] researched the structure-PZT coupling resistance through experiments and derived a simple PZT-driven coupling admittance expression.

Soh et al. [16] have done a great deal of experimental research on micro-damage detection in civil engineering structures and found that non-parametric index using Root-Mean-Square Deviation (RMSD) correlated well with the damage progression in the structure. Since then Soh and Bhalla [17] have also developed a fuzzy conceptual model that can quantitatively demonstrate the degree of damage in concrete by using the amplitude of change of structural equivalent stiffness. In addition, Annamdas and Soh [18] present a new embedded PZT patch and have done a great deal of experimental research on micro-damage detection in civil engineering structures and found that the micro-cracks of concrete structure can be detected by using electro-mechanical impedance method. After that, Lim et al. [19] proposed a new method for damage diagnosis from the measured admittance signatures in terms of equivalent structural parameters. Then Bhalla and Soh [20] present a new method of damage diagnosis by changing the structural impedance signal at high frequencies using PZT patches. Tseng and Naidu [21] used some simple structures to find the impedance relationship between the PZT and the structure, and confirmed the feasibility of the electro-mechanical impedance approach. The feasibility of using impedance-based non-destructive testing to identify damage in concrete was also verified [22]. Based on

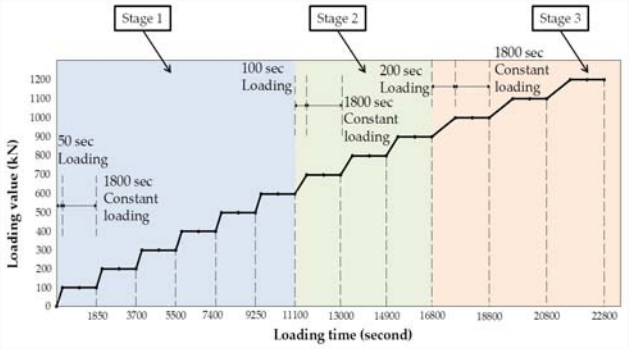

Figure 8: Loading method of the experiment.

Figure 9: Picture of crashed specimen.

smart Piezoelectric Transducer (PZT) patches, Tseng and Wang [23] further developed a modeling framework to determine the structural impedance response and the dynamic output forces of PZT patches from the electric admittance measurements. Park et al. [24] obtained plenty of results by using PZT sensors to monitor the mechanical properties of concrete structures. They found that electro-mechanical impedance methods can be used to identify the degree of structural damage in harsh environments and the sensitivity of electro-mechanical impedance based micro-damage monitoring have been verified [25]. In order to remove the effects of temperature factor from the changes of PZT impedance signals caused by structural damage, Park et al. [26,27] designed an algorithm that incorporated temperature compensation into the piezoelectric impedance approach to assure its practical application.

Furthermore, Dumoulin et al. [28] used SAs to investigate and compare different damage indicators in a reinforced concrete beam subjected to three-point bending test. Karaiskos et al. [29] also focused on ultrasonic wave propagation techniques by using embedded piezoelectric transducers for online monitoring of concrete and demonstrated the performance of the system which is able to detect the cracking until complete failure.

In addition, Ayres et al. [30] addressed electro-mechanical impedance measurements from experimental structures and a subsequent statistical method for quantitatively determining the classification of "damaged". A potentially powerful tool for damage detection and health monitoring named E/M impedance technique was demonstrated by Giurgiutiu et al. [31]. Yang et al. [32] employed smart Optical Fiber Sensor (OFS) and lead zirconate titanate (PZT) impedance sensor for comprehensive health monitoring of rocks. Yang et al. [33] developed a reusable PZT transducer setup for monitoring the initial hydration of concrete and structural health

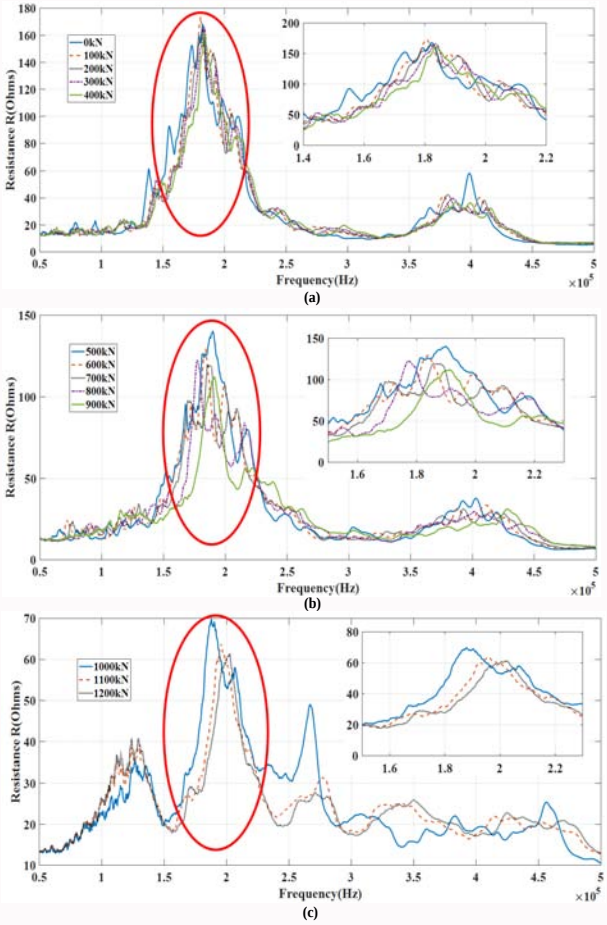

Figure 10: Electrical impedance signature of group one acquired from the SA (real part of the impedance signal). (a) 0 kN to 400 kN; (b) 500 kN to 900 kN; (c) 1000 kN to 1200 kN.

monitoring. The feasibility of the EMI sensing technique for the real time strength development of early-age concrete was investigated by Shin and Oh [34]. Park et al. [35] explored the capability of the E/M impedance status monitoring of pipeline structure after earthquake. Park et al. [36] summarized the hardware and software issues of impedance-based structural health monitoring based on piezoelectric materials. Park et al. [37] developed an EMI based SHM approach using modified auto-regressive model with exogenous inputs (ARX). Wang et al. [38] extended the impedance method to timber specimens for damage detection. All of these researches demonstrated that the electro-mechanical impedance approach is a promising way to monitor the healthy state of structures.

In our previous studies, the influence of axial force on properties of steel fiber reinforced concrete in elastic stage was investigated [39]. Experimental results demonstrated that the axial load has a great influence on EMI value, and further, there is a great linearity between the normalized-RMSD and the applied loading, shown in Figure 1.

According to the axial forces influence of steel fiber concrete within the elastic range of strains, further investigation about the ultimate load influence was carried out in this paper. The E/M impedance method was used to detect the damage status of steel fiber concrete. Step-by-step loading case was conducted, which can clearly show the axial loading effect during elastic, plastic and the destruction stage of steel fiber concrete. The normalized RMSD-based analysis

which proposed in the earlier paper of elastic range of strains was also applied. The test results show that the normalized RMSD was gradually increased with the increase of axial load. The normalized RMSD-based index is effect to monitor the damage status of steel fiber concrete.

Piezoceramic Based Smart Aggregate (SA)

Smart aggregate is a kind of PZT based sensor which made by sandwiched the waterproofed PZT into the marble protection. Because of the piezoelectric properties [40], smart aggregates can be used as sensor in this experiment. Figure 2(a) shows the detail information about smart aggregate. A fragile PZT connected with lead wire was embedded in the center of the marble protection to prevent sudden damage. The dimension of the PZT (D_{33}) is 15 mm × 15 mm square. The diameter of the smart aggregate is 25 mm, and the height is 20 mm. Figure 2(b) shows a photo of a fabricated smart aggregate and an exploded view of it. Smart aggregates have been used in concrete structure health monitoring research; for example, Yan et al. [41] applied smart aggregates to the damage monitoring of the shear wall under repeated load and found that the smart aggregate can determine the damage area of the shear wall.

Electro-Mechanical (E/M) Impedance and Normalized Root-Mean-Square-Deviation (RMSD) Approach

Electro-mechanical impedance method, which diagnoses damage by comparing the E/M impedance of smart aggregates before and after damage happens, is a promising new technique for damage detection [42]. In this paper, the SA was casted into the center of concrete specimen, once the damage occurred, the natural frequencies of the whole structure changes, thereby further causing the change of E/M impedance [43,44]. Therefore, the E/M impedance signal measured by the smart aggregates can be used to diagnosis and detect the damage status of structure. In addition, it can further perform the damage diagnosis and the health monitoring on various structures. In electronic electrodynamics, admittance is defined as the reciprocal of impedance. The formula of admittance, which is shown in Equation (1), can be derived according to the equilibrium equation, the piezoelectric equation and the wave equation [45]. Equation (2) shows the formula of impedance derived from the formula of admittance.

$$Y = i\omega \frac{w_A l_A}{h_A}\left[\bar{\varepsilon}_{33}^{\sigma} - \frac{Z_S}{Z_S + Z_A} d_{31}^2 \bar{Y}_{22}^{E}\right] \quad (1)$$

$$Z(\omega) = \frac{1}{Y} = \frac{h_A}{i\omega w_A l_A}\left(\bar{\varepsilon}_{33}^{\sigma} - \frac{Z_S}{Z_S + Z_A} d_{31}^2 \bar{Y}_{22}^{E}\right)^{-1} \quad (2)$$

where, Y is admittance, ω is the angular frequency of excitation. i is imaginary unit. w_A, h_A, l_A are respectively the PZT's width, thickness and length. $\bar{\varepsilon}_{33}^{\sigma}$ is the complex permittivity when PZT's stress is zero or a constant. d_{31} is piezoelectric constant and $\bar{Y}_{22}^{E}$ is complex Young's modulus at zero or constant electric field. Z_A and Z_S are representing PZT's mechanical impedance and structure's mechanical impedance respectively.

A normalized RMSD-based analysis is developed to process the impedance signal. RMSD has been widely used in data processing. The basic idea of RMSD (Root-Mean-Square Deviation) is to compare the arithmetic square root under different status of the same data with each other. By using RMSD, the structural information in different status is compared to the information in the non-destructive status to obtain the structural damage. The equation of RMSD and the equation of normalized-RMSD are shown in Equation (3) and Equation (4), respectively.

$$RMSD = \sqrt{\frac{\sum_N (Z_i^1 - Z_i^0)^2}{\sum_N (Z_i^0)^2}} \times 100\% \quad (3)$$

$$NI = \frac{I_{RMSD}^{i} - I_{RMSD}^{w}}{I_{RMSD}^{l} - I_{RMSD}^{w}} \quad (4)$$

where, Z^1 is the impedance of a measuring point at a single frequency and Z^0 is the reference value of the same frequency at 100 kN. I^i_{RMSD} is the RMSD index at *ith* loading condition in the experiment. I^w_{RMSD} is the RMSD index of the specimen under no-loading condition. I^l_{RMSD} is the RMSD index with the largest load applied. Although RMSD have been employed to associate the damage level with the changes in the impedance value, it is difficult to determine the location of damage using such methods [46].

Experiment Preparation and Experimental Setup

This section describes the steel fiber concrete that will be used to demonstrate the smart aggregate based impedance method for destruction monitoring. In addition, the experimental setup involves the device we used and the loading method.

Steel fiber concrete specimen

The concrete mix proportions are shown in Table 1. Table 2 shows that steel fiber concrete specimens were divided into five groups based on the different content of steel fiber. The steel fiber we used in concrete specimen is shown in Figure 3. Every group has three specimens. All the concrete specimens are the same size, which is 150 mm × 150 mm × 150 mm. For each specimen, a smart aggregate is embedded in the center of the specimen, as shown in Figure 4. Figure 5 shows the photo of the specimen.

Experimental setup

Testing schematic and devices are shown in Figure 6 and 7. A compression testing machine (YAW-3000A) was used to load the concrete specimens. Step-by-step load is used to apply the axial load. A precision impedance analyzer (Agilent 4294A) was used to detect the impedance signal of the structure. The precision impedance analyzer

Table 1: Proportions of concrete mix (kg/m³).

Cement (PO42.5)	sand	stone	water	fly ash	water-reducing admixture
400	740	1100	150	50	7.4

Table 2: The groups of steel fiber concrete.

Groups	1st	2nd	3rd	4th	5th
Specimen's number	1-1,1-2,1-3	2-1,2-2,2-3	3-1,3-2,3-3	4-1,4-2,4-3	5-1,5-2,5-3
The content of steel fiber (kg/m³)	0	30	60	90	120

Table 3: Loading method of the experiment.

Loading range (kN)		0-600	600-900	900-destruction
Loading gradient (kN)		100	100	100
Loading speed (kN/s)		2	1	0.5
Loading time (s)	**Gradient loading time**	50	100	200
	Gradient maintaining time	1800	1800	1800

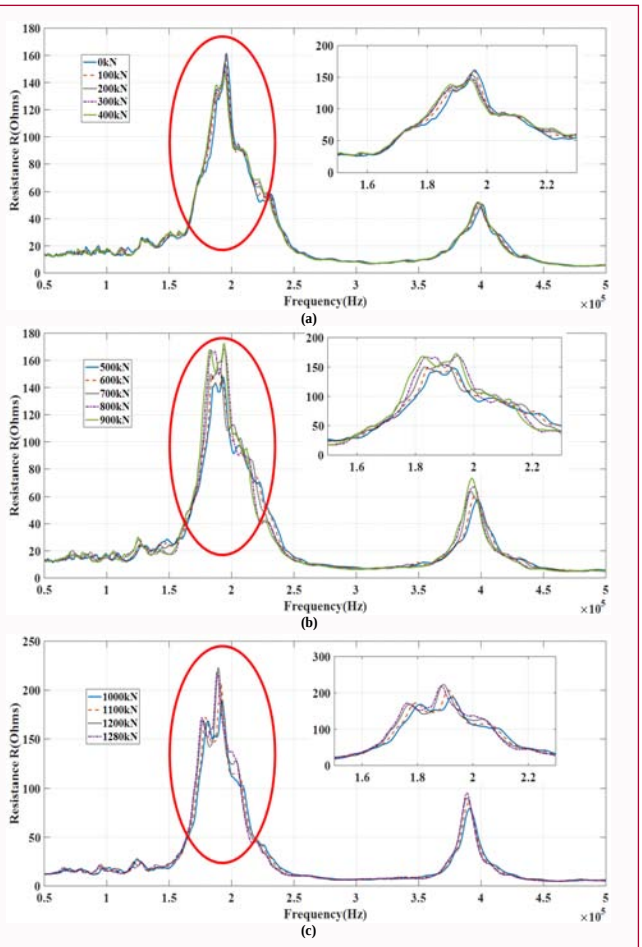

Figure 11: Electrical impedance signature of group two acquired from the SA (real part of the impedance signal). (a) 0 kN to 400 kN; (b) 500 kN to 900 kN; (c) 1000 kN to 1280 kN.

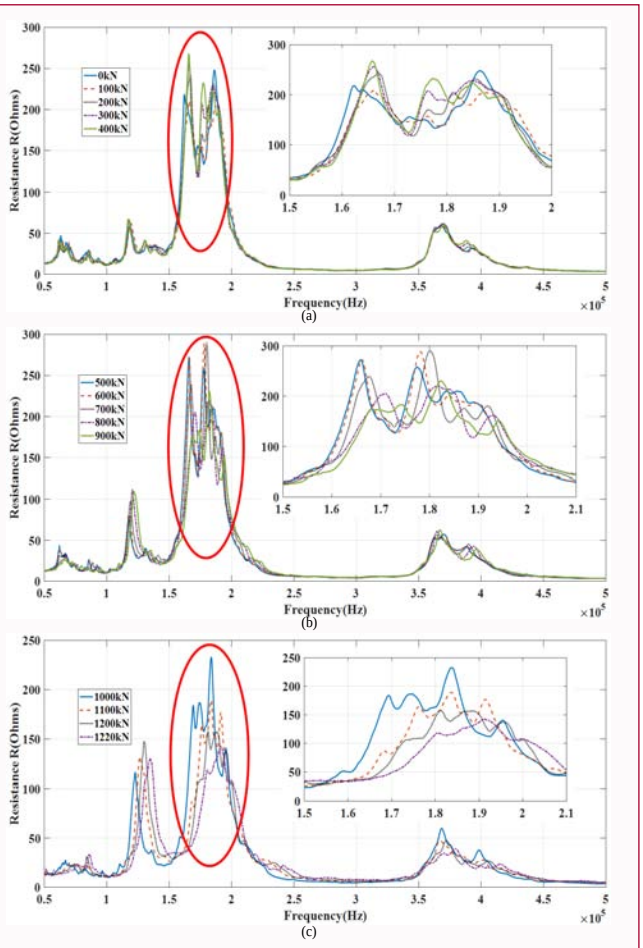

Figure 12: Electrical impedance signature of group three acquired from the SA (real part of the impedance signal). (a) 0 kN to 400 kN; (b) 500 kN to 900 kN; (c) 1000 kN to 1220 kN.

applies high frequency AC voltage to smart aggregate actuator, which causes the actuator to generate high-frequency vibration and give mechanical waves inside the structure. The sweep frequency ranges of the impedance signal 100 kHz to 500 kHz. The real parts of the E/M impedance signals were record to measure the influence of ultimate axial force on destruction of steel fiber concrete.

Experiment Preparation and Experimental Setup

Experimental procedures

As shown in Table 3 and 8, the process of the experiment can be divided into three phases. A teach maintaining stage, the loading level was maintained constant for 30 min. The impedance signals were measured at every beginning, midpoint and ending of the maintaining time. In the first phase, the loading speed of the specimens was 2 kN/s and the loading level was maintained constant at 100, 200, 300, 400, 500 and 600 kN. In the second phase, the load increase with a rate of 1 kN/s. The loading level maintained constant at 700, 800 and 900 kN, respectively. In the last phase, the loading speed was 0.5 kN/s until the specimen was fully damaged. The maintaining process was at integral hundreds digits.

Experimental results and discussion

Figure 9 shows the picture of crashed specimen in this experiment. As shown in Figures 10-14, we can see there is no consistent relationship between force and amplitude of impedance. Although the amplitude of impedance can be considered as chaotically increasing as the force increases (group two, group four and group five) and it is hard to reach an agreement on every cases (group one and group three). As the force increases, the corresponding frequency of the amplitude of impedance also shows a chaotically trend. We cannot get an explicit relationship between the steel fiber concrete destruction process and the real part of the impedance signal. In order to show the relationship between axial load and impedance signal more clearly, the normalized RMSD index was calculated at

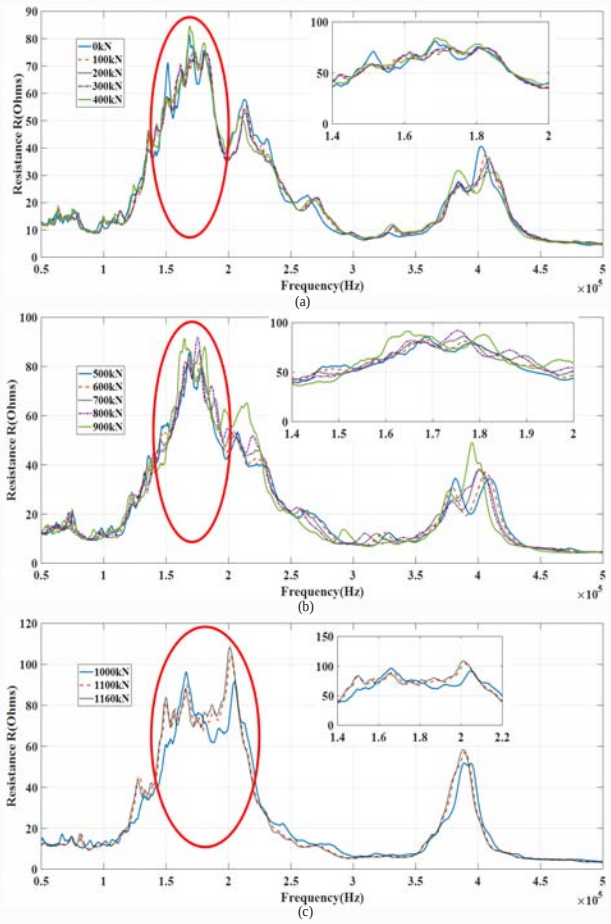

Figure 13: Electrical impedance signature of group four acquired from the SA (real part of the impedance signal). (a) 0 kN to 400 kN; (b) 500 kN to 900 kN; (c) 1000 kN to 1160 kN.

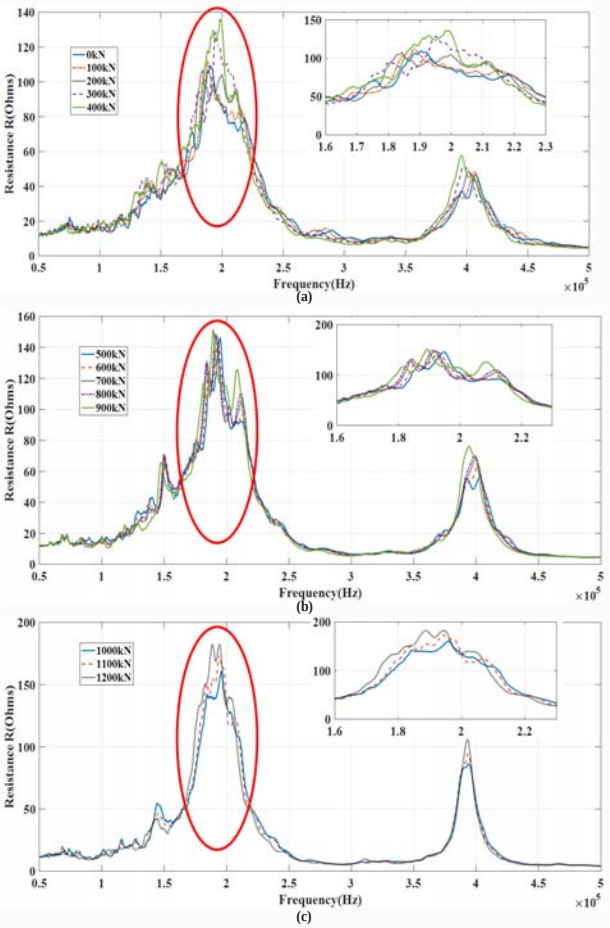

Figure 14: Electrical impedance signature of group five acquired from the SA (real part of the impedance signal). (a) 0 kN to 400 kN; (b) 500 kN to 900 kN; (c) 1000 kN to 1200 kN.

each measuring points, the authors draw them into a histogram, which showed in Figures 15-19.

Generally, the normalized RMSD index increase with increasing load in Figures 15-19. As aforementioned, this paper mainly focused on the plastic stage and destruction stages. Therefore, the impedance of a measuring point at 100 kN was set as a reference value. As shown in the Figure 19, the normalized RMSD started from 200 kN. In order to eliminate the random errors caused by unstable random factors, we average the RMSD of each group. And we can clearly see from the figures that the normalized RMSD index of steel fiber concrete will increase by a large margin near the time of destruction. The normalized RMSD index can be effectively used to monitor the steel fiber concrete destruction process and predict the destruction of steel fiber concrete.

With further analysis, the reasons of the date fluctuation are mainly caused by following aspects. Firstly, the stress redistribution around SA leads to irregular voltage signals due to the direct piezoelectric effect. Secondly, the SA sensors receive the acoustic signals, which caused by the opening and closure of cracks, as well as the sensing signals, which complicate the wave forms. Thirdly, the uneven distribution of the steel fibers in the steel fiber concrete makes the distribution of the cracks uneven, which result in some differences between the specimens. Fourthly, concrete vibrating leads to slight deviation of smart aggregates, thus affecting the receiving

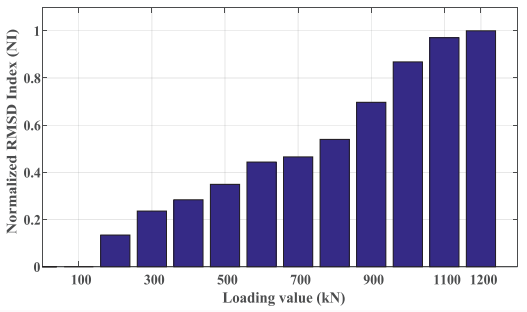

Figure 15: The NI-RMSD index of group one.

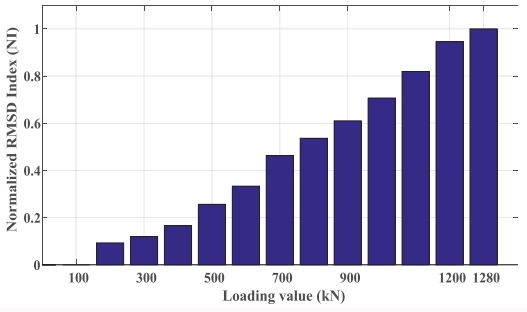

Figure 16: The NI-RMSD index of group two.

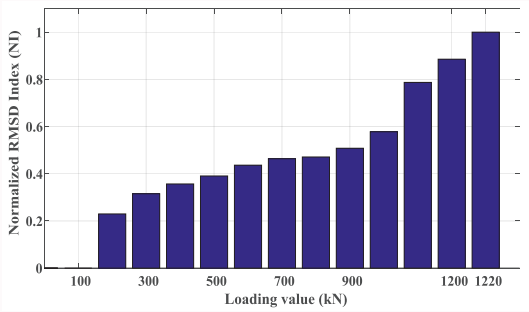

Figure 17: The NI-RMSD index of group three.

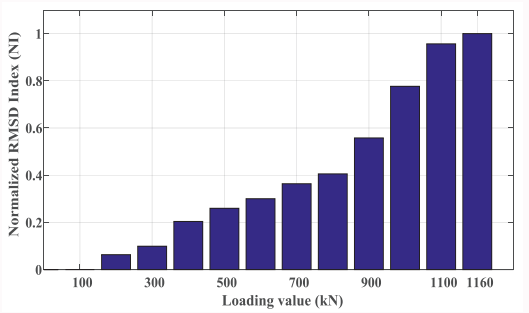

Figure 18: The NI-RMSD index of group four.

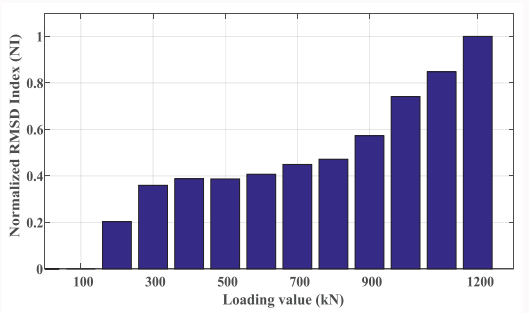

Figure 19: The NI-RMSD index of group five.

signal amplitude.

Conclusion

The proposed piezoceramic based impedance method was experimentally proven to be is liable approach in health monitoring and further monitoring the damage status of steel fiber concrete. Impedance method can be used to measure the impact of axial load on the steel fiber concrete. Since smart aggregates were embedded into steel fiber concrete, the process of crack development can be monitored by using impedance method. In addition, a normalized RMSD-based analysis is developed to process the data. It can be seen that with the increase of the axial load, the normalized RMSD index is gradually increased. Therefore, the effect of axial loads on steel fiber concrete can be clearly demonstrated by normalized RMSD.

Acknowledgment

This work was supported by the Major State Basic Research Development Program of China (973 Program, grant number 2015CB057704). The authors would like to thank for the financial supports.

References

1. Bafghi MB, Amini F, Nikoo HS, Sarkardeh H. Effect of steel fiber and different environments on flexural behavior of reinforced concrete beams. Applied Sciences. 2017;7(10):1011.
2. Swamy RN, Al-Noori K. Flexural properties of steel fibre reinforced concrete. Concrete. 1975;9(6):30-1.
3. Swamy RN, Lankard DR. Some practical applications of steel fibre reinforced concrete. Proceedings of the Institution of Civil Engineers. 1974;56(3):235-56.
4. De Moura JDRV, Steffen V. Impedance-based health monitoring for aeronautic structures using statistical meta-modeling. J Intell Mater Syst Struct. 2006;17(11):1023-36.
5. Xing KJ, Fritzen CP. Monitoring of growing fatigue damage using the e/m impedance method. Key Engineering Materials. 2007;347:153-8.
6. Boukabache H, Escriba C, Zedek S, Medale D, Rolet S, Fourniols JY. System-on-chip integration of a new electromechanical impedance calculation method for aircraft structure health monitoring. Sensors (Basel). 2012;12(10):13617-35.
7. Zhang J, Zhang C, Xiao J, Jiang J. A PZT-based electromechanical impedance method for monitoring the soil freeze–thaw process. Sensors (Basel). 2019;19(5):1107.
8. Song G, Gu H, Mo YL. TOPICAL REVIEW: Smart aggregates: multi-functional sensors for concrete structures—a tutorial and a review. Smart Mater Struct. 2008;17(3):033001.
9. Gu H, Song G, Dhonde H, Mo YL, Yan S. Concrete early-age strength monitoring using embedded piezoelectric transducers. Smart Mater Struct. 2006;15(6):1837.
10. Song G, Olmi C, Gu H. An overheight vehicle bridge collision monitoring system using piezoelectric transducers. Smart Mater Struct. 2007;16(2):462-8.
11. Song G, Mo YL, Otero K, Gu H. Health monitoring and rehabilitation of a concrete structure using intelligent materials. Smart Mater Struct. 2006;15(2):309.
12. Du G, Zhang J, Zhang J, Song G. Experimental study on stress monitoring of sand-filled steel tube during impact using piezoceramic smart aggregates. Sensors (Basel). 2017;17(8):1-17.
13. Liang C, Sun FP, Rogers CA. An impedance method for dynamic analysis of active material systems. J Intell Mater Syst Struct. 1997;8(4):323-34.
14. Liang C, Sun FP, Rogers CA. Electromechanical impedance modeling of active material systems. Smart Mater Struct. 1996;5(2):171.
15. Liang C, Sun FP, Rogers CA. Coupled electromechanical analysis of adaptive material systems-determination of the actuator power consumption and system energy transfer. J Intell Mater Syst Struct. 1997;8(4):335-43.
16. Soh CK, Tseng KKH, Bhalla S, Gupta A. Performance of smart piezoceramic patches in health monitoring of a RC bridge. Smart Mater Struct. 2000;9(4):533.
17. Soh CK, Bhalla S. Calibration of piezo-impedance transducers for strength prediction and damage assessment of concrete. Smart Mater Struct. 2005;14(4):671.
18. Annamdas VGM, Soh CK. Embedded piezoelectric ceramic transducers in sandwiched beams. Smart Mater Struct. 2006;15(2):538.
19. Lim YY, Bhalla S, Soh CK. Structural identification and damage diagnosis using self-sensing piezo-impedance transducers. Smart Mater Struct. 2006;15(4):987.
20. Bhalla S, Soh CK. Structural impedance based damage diagnosis by piezo-transducers. Earthq Eng Struct Dyn. 2003;32(12):1897-916.
21. Tseng KKH, Naidu ASK. Non-parametric damage detection and

characterization using smart piezoceramic material. Smart Mater Struct. 2002;11(3):317.

22. Tseng KK. Impedance-based non-destructive and non-parametric infrastructural performance evaluation. Experimental Mechanics. 2004;44(1):109-12.

23. Tseng KK, Wang L. Impedance-based method for nondestructive damage identification. J Eng Mech. 2005;131(1):58-64.

24. Park G, Cudney HH, Inman DJ. Impedance-based health monitoring of civil structural components. Journal of Infrastructure Systems. 2000;6(4):153-60.

25. Allen DW, Peairs DM, Inman DJ. Damage detection by applying statistical methods to PZT impedance measurements. Proc SPIE. 2004.

26. Park G, Cudney HH, Inman DJ. Removing effects of temperature changes from piezoelectric impedance-based qualitative health monitoring. Proc SPIE. 1998;3330:103-14.

27. Park G, Kabeya K, Cudney HH, Inman DJ. Impedance-based structural health monitoring for temperature varying applications. JSME Int J. 1999;42(2):249-58.

28. Dumoulin C, Karaiskos G, Deraemaeker A. Monitoring of crack propagation in reinforced concrete beams using embedded piezoelectric transducers. International Conference on Fracture Mechanics of Concrete and Concrete Structures. 2013.

29. Karaiskos G, Flawinne S, Sener JYS, Deraemaeker A. Design and validation of embedded piezoelectric transducers for damage detection applications in concrete structures. Key Engineering Materials. 2013;569-570;805-11.

30. Ayres JW, Lalande F, Chaudhry Z, Rogers CA. Qualitative impedance-based health monitoring of civil infrastructures. Smart Mater Struct. 1998;7(5):599-605.

31. Giurgiutiu V, Reynolds A, Rogers CA. Experimental investigation of E/M impedance health monitoring for spot-welded structural joints. J Intell Mater Syst Struct. 1999;10(10):802-12.

32. Yang Y, Annamdas VG, Wang C, Zhou Y. Application of multiplexed FBG and PZT impedance sensors for health monitoring of rocks. Sensors (Basel). 2008;8(1):271-289.

33. Yang Y, Divsholi BS, Kiong SC. A reusable PZT transducer for monitoring initial hydration and structural health of concrete. Sensors (Basel). 2010;10(5):5193-208.

34. Shin SW, Oh TK. Application of electro-mechanical impedance sensing technique for online monitoring of strength development in concrete using smart PZT patches. Construction & Building Materials. 2009;23(2):1185-8.

35. Park G, Cudney HH, Inman DJ. Feasibility of using impedance-based damage assessment for pipeline structures. Earthq Eng Struct Dyn. 2001;30(10):1463-74.

36. Park G, Sohn H, Farrar CR, Inman DJ. Overview of piezoelectric impedance-based health monitoring and path forward. Shock and Vibration Digest. 2003;35(6):451-63.

37. Park G, Rutherford AC, Sohn H, Farrar CR. An outlier analysis framework for impedance-based structural health monitoring. J Sound Vib. 2005;286(1-2):229-50.

38. Wang D, Wang Q, Wang H, Zhu H. Experimental study on damage detection in timber specimens based on an electromechanical impedance technique and RMSD-based mahalanobis distance. Sensors. 2016;16(10):1-17.

39. Wang Z, Chen D, Zheng L, Huo L, Song G. Influence of axial load on Electromechanical Impedance (EMI) of embedded piezoceramic transducers in steel fiber concrete. Sensors (Basel). 2018;18(6):1-17.

40. Wang J, Kong Q, Shi Z, Song G. Electromechanical properties of smart aggregate: theoretical modeling and experimental validation. Smart Mater Struct. 2016;25(9):095008.

41. Yan S, Sun W, Song G, Gu H, Huo LS, Liu B, et al. Health monitoring of reinforced concrete shear walls using smart aggregates. Smart Mater Struct. 2009;18(4):047001.

42. Yang Y, Hu Y, Lu Y. Sensitivity of PZT impedance sensors for damage detection of concrete structures. Sensors (Basel). 2008;8(1):327-46.

43. Annamdas VGM, Yang Y, Soh CK. Influence of loading on the electromechanical admittance of piezoceramic transducers. Smart Mater Struct. 2007;16(5):1888.

44. Ong CW, Yang Y, Naidu ASK, Lu Y, Soh CK. Application of the electromechanical impedance method for the identification of in-situ stress in structures. Proc SPIE. 2002;4935:485621.

45. Sun FP, Chaudhry Z, Liang C, Rogers A. Truss structure integrity identification using PZT sensor-actuator. J Intell Mater Syst Struct. 1994;6(1):134-9.

46. Yang Y, Divsholi BS. Sub-frequency interval approach in electromechanical impedance technique for concrete structure health monitoring. Sensors (Basel). 2010;10(12):11644-61.